VIII International Conference on Textile Composites and Inflatable Structures
STRUCTURAL MEMBRANES 2017
K.-U.Bletzinger, E. Oñate and B. Kröplin (Eds)

ISOGEOMETRIC ANALYSIS FOR STAGED CONSTRUCTION WITHIN LIGHTWEIGHT DESIGN

ANNA M. BAUER, ROLAND WÜCHNER AND KAI-UWE BLETZINGER

Lehrstuhl für Statik
Technische Universität München
Arcisstr. 21, 80333 München, Germany
e-mail: am.bauer@tum.de, web page: http://www.st.bgu.tum.de

Key words: Lightweight Structures, Staged Construction, Hybrid Structures, Isogeometric Analysis, Embedding, Nonlinear Kinematics

Abstract. Hybrid, bending-active structures constitute a challenging task for structural design due to the high dependency between shape and forces. Isogeometric analysis suggests itself in this context because of several advantages. Model conversion with concomitant corruption of the simulation results can be overcome. All stages of the construction, which are necessary for the correct simulation of such structures, can be modeled and correctly linked. Moreover, the parameter space of the NURBS description provides a perfectly suited, additional design space for embedded entities, which can be defined independently of the parametrization.

The contribution of this paper is a presentation of the basics for embedding within isogeometric analysis and reveals beneficial aspects of nested NURBS descriptions in the context of staged construction. A case study of a staged simulation is carried out and another one for the form-finding procedure of hybrid structures.

1 INTRODUCTION

The development of an aesthetic and robust design in lightweight design is a challenging task. Architects and engineers are required to work closely together since their decisions directly influence each other. Load bearing behavior of lightweight design is form dominated. Or to put it differently, an appropriate shape design results in a good load bearing behavior and therefore the need for less material. Lightweight design uses flexible components which form a resistant structure after forming, straining and assembling. Since the actual construction is an essential part of the resulting stiffness, it is important to also include the different stages into the simulation.

Isogeometric Analysis (IGA), as defined in [1], has several aspects, which are beneficial for lightweight design. First of all, it uses smooth Non-uniform rational B-Splines

(NURBS) as basis functions. The geometric properties are not corrupted by the polygon mesh of a classic FE-analysis. The analysis and its results can be incorporated into CAD, where several well-suited tools for the modeling of further stages, such as the derivation of a surface description from boundary curves, are available. Furthermore, NURBS patches provide a huge parameter space for the parametric design. Meshing does not subdivide the patches and the model can be modified without taking care of the meshing of interacting members. Therefore, it is very convenient to apply IGA for the definition of the interaction of single components. The parameter space can also be used for a description of embedded entities. The embedding can be realized by another NURBS description in the parameter space of the master NURBS patch. The idea stems from the trimming of CAD geometries. Here, the borders of a trimmed surface are described by curves in its parameter space. These edge curves were applied by Breitenberger et al. [2] for trimming in isogeometric B-Rep analysis (IBRA) and for coupling of multipatches as well as for edge cables by Philipp *et al.* [3]. However, such a description can also be used within the surface and be enhanced with further structural properties. The geometric description of the continuum of a one-dimensional element is then adapted to the nested NURBS description. Further derivations of structural element formulations are then analogue to the surface-independent element formulation.

Therefore, this contribution is outlined as follows. Section 2 presents essential aspects of the simulation of staged construction. The above mentioned embedding within NURBS is explained in Section 3. A transfer to structural analysis is shown briefly for the element formulation of an embedded beam in Section 4. These two separate topics are brought together in two detailed application examples in Section 5.

2 STAGED CONSTRUCTION

A staged construction is still a challenge in the computer simulation. This is especially true, if some structural configurations are derived from previous results of other parts. Here, one can benefit a lot of the CAD facilities. Constructing a surface from boundary lines is for example quite effortless in CAD systems whereas it is hardly possible in a FE-kernel with a non-matching parametrization. Intermediate steps with CAD recovery are part of the classical workflow which influences the accuracy of the results, since the link between the two FE models is corrupted if the parametrization cannot be retained. In contrast, the parametrization is preserved with isogeometric analysis by retaining the basis function between CAD modeling and simulation or when needed by exactly transferring to a refined configuration.

The two usual approaches for the consideration of previous simulations are either transferring stresses on integration points (*InitStress*) or displacements of nodes (*InitDisp*). The transferred quantity is then applied as initial condition. The methods are compared for a tension test of a shell (see Fig. 1). The shell strip, modeled by a Kirchhoff-Love shell [4], is vastly stretched in two steps by increased load λP and then unloaded. Note that this simulation problem is easily solved within one simulation, since the structure is not

modified. The one-simulation result serves as reference. Simulation 1 is now interrupted after solving $\lambda = 1$ and a second simulation is started for every approach. The initial configuration ($\lambda = 1$) is in equilibrium for both approaches, but a significant difference can be observed while further loading or unloading in simulation 2. The *InitStress* method differs from the reference solution for $\lambda = 2$ and in the unloaded state ($\lambda = 0$), whereas the *InitDisp* method perfectly matches. Further details can be found in the contribution of Dieringer *et al.* [5]. Only the capturing of previous simulation by initial displacement of the nodes resp. control points is suitable for statically nonlinear application, which is usually necessary for hybrid structures.

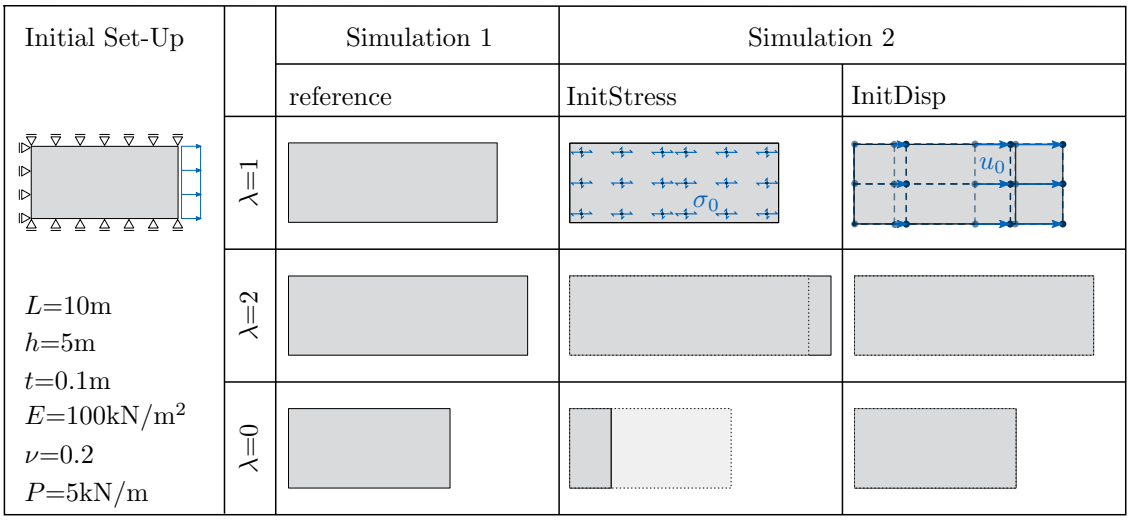

Figure 1: Comparison of the two methods *InitStress* and *InitDisp* for simulating staged construction. Note that the computation was carried out with better refinement, *i.e.* more Gauss points and control points, than illustrated. The reference solution is added for simulation 2 with dotted lines.

3 EMBEDDING WITHIN NURBS GEOMETRIES

A further advantage of isogeometric analysis is the relatively huge parameter space, which is not subdivided throughout the simulation. Note that a respectively huge parameter space with "classic" low order finite elements, *i.e.* huge elements, is accompanied by a loss of accuracy. In the following, the usually used basis function, *Non-Uniform Rational B-Splines* (NURBS), of IGA are recalled briefly. NURBS provide in general a description for smooth surfaces and curves in CAD systems by a discrete number of control points $\mathbf{P}$ with weight w, a knot vector and a polynomial degree p resp. q. The geometry description $\mathbf{C}(\xi)$ or $\mathbf{S}(\xi, \eta)$ is then derived by the product of the control points and their basis function R.

$$\mathbf{C}(\xi) = \sum_{i=1}^{n} R_{i,p}(\xi)\mathbf{P}_i \qquad\qquad \mathbf{S}(\xi,\eta) = \sum_{i=1}^{n}\sum_{j=1}^{m} R_{ij,pq}(\xi,\eta)\mathbf{P}_{ij}\ , \tag{1}$$

The basis function R is derived by weighting the underlying B-Spline basis functions N resp. M, which in turn are defined by the knot vector and polynomial degree. Details on the computation of B-Splines and NURBS can be found in the contribution of Piegl and Tiller [6].

$$R_{i,p}(\xi) = \frac{N_{i,p}(\xi)w_i}{\sum_{j=1}^{n} N_{j,p}(\xi)w_j} \qquad R_{ij,pq}(\xi,\eta) = \sum_{i=1}^{n}\sum_{j=1}^{m} \frac{N_{i,p}(\xi)M_{j,q}(\eta)w_{ij}}{\sum_{k=1}^{n}\sum_{l=1}^{m} N_{k,p}(\xi)M_{l,q}(\eta)w_{kl}} \tag{2}$$

The parameter space spanned by a NURBS description is now taken as an additional design space. Entities which are related to a specific location on a NURBS geometry are described by a NURBS description in the respective parameter space, called the super domain. This is exemplified for a line element embedded in a surface. As a consequence, the local line is expressed by the control parameters (degrees of freedom) of the super domain. Hence, explicit coupling is avoided. All quantities which refer to the parameter space of the super domain will henceforth be denoted with $\overline{(\bullet)}$.

$$\overline{\mathbf{C}}(\bar{\xi}) = \begin{pmatrix} \xi\left(\bar{\xi}\right) \\ \eta\left(\bar{\xi}\right) \end{pmatrix} = \sum_{\bar{i}=1}^{n} R_{\bar{i},\bar{p}}(\bar{\xi})\overline{\mathbf{P}}_{\bar{i}} \tag{3}$$

The description of lines in the parameter space can be derived either manually, *i.e.* by directly defining the curve in the parameter space, or by using the CAD-implemented surface-to-surface intersection (SSI) algorithms of *e.g.* [7, 8, 9, 10] for larger and more complex tasks. Note that the precision of the mapping into the parameter space is strongly dependent on the CAD tolerances.

The embedded structural properties can be derived from the curve description in the geometry space. Every term in the embedded curve is described by the control points of the surface. If further quantities have to be described, additional control variables (DOFs) can be added to the control points of the surface, which belong to the knot spans crossed by the curve.

$$\begin{aligned} \mathbf{C}(\bar{\xi}) &= \sum_{i=1}^{n}\sum_{j=1}^{m} R_{ij,pq}\left(\bar{\xi}\right)\mathbf{P}_{ij} = \sum_{i=1}^{n}\sum_{j=1}^{m} R_{ij,pq}\left(\xi\left(\bar{\xi}\right),\eta\left(\bar{\xi}\right)\right)\mathbf{P}_{ij} \\ &= \sum_{i=1}^{n}\sum_{j=1}^{m} R_{ij,pq}\left(\sum_{\bar{i}=1}^{\bar{n}} R_{\bar{i},\bar{p}}\left(\bar{\xi}\right)\overline{\mathbf{P}}_{\bar{i}}\right)\mathbf{P}_{ij} \end{aligned} \tag{4}$$

An overview of all presented geometry descriptions within the proposed workflow is given in Fig. 2.

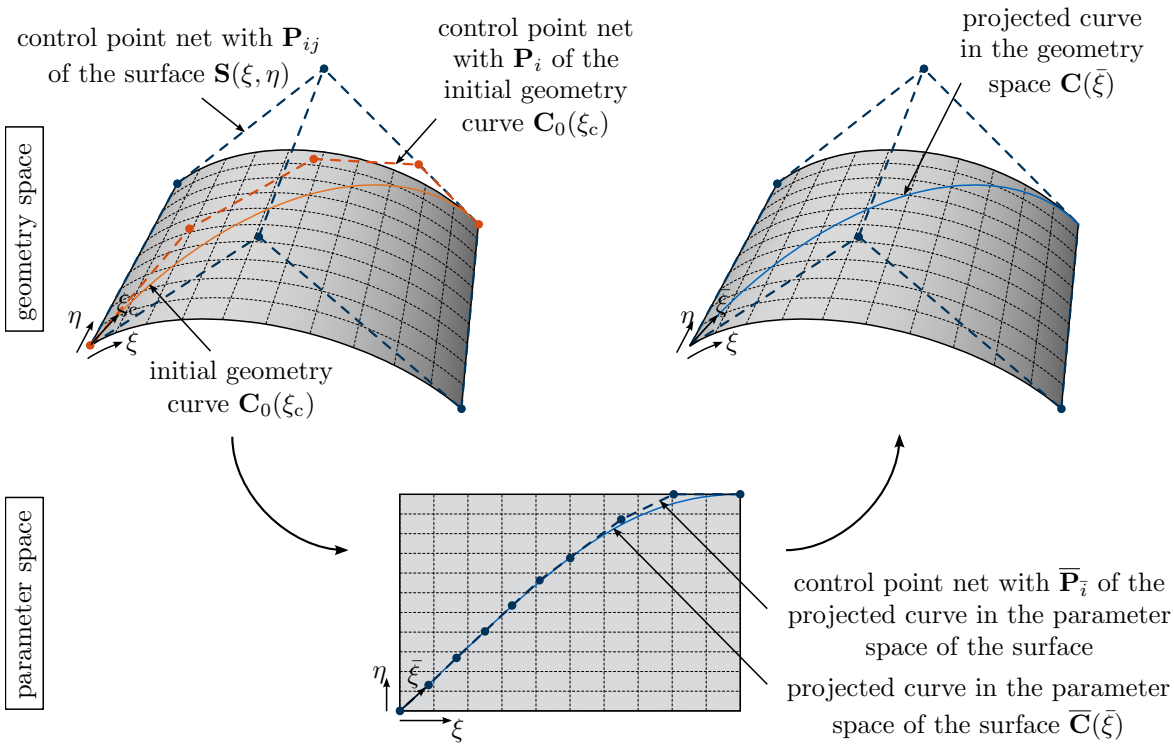

Figure 2: Overview of the presented geometry descriptions.

4 EMBEDDED BEAM ELEMENT FORMULATION

A brief overview of the derivation of the structural element formulation of the embedded beam as proposed in [11] is presented as a template for further formulations based on the embedded curve description. The derivation is based on the *Principle of Virtual Work*. Let Ω be the undeformed super domain and $\partial\Omega$ be the boundary. Additional terms in the work expression are derived from the sub domain of the embedded curve Ω_C and its respective boundary $\partial\Omega_\mathrm{C}$. The second Piola-Kirchhoff (PK2) stresses are assigned by $\mathbf{S}$ and the energetically conjugated virtual Green-Lagrange (GL) strains related to the virtual displacement $\delta\mathbf{u}$ by $\delta\mathbf{E}$. The external work consists of body forces $\mathbf{B}$ and boundary forces $\mathbf{t}$ times their respective virtual displacement. The material density is denoted as ρ_0.

$$\delta W = -\delta W_\mathrm{int} + \delta W_\mathrm{ext} = -\int_\Omega \mathbf{S}^\mathrm{S} : \delta\mathbf{E}^\mathrm{S}\, dx \; - \int_{\Omega^\mathrm{C}} \mathbf{S}^\mathrm{C} : \delta\mathbf{E}^\mathrm{C}\, dx \tag{5}$$
$$+ \left(\int_{\partial\Omega} \mathbf{t}^\mathrm{S} : \delta\mathbf{u}^\mathrm{S}\, dx + \int_{\Omega^\mathrm{S}} \rho_0 \mathbf{B}^\mathrm{S} : \delta\mathbf{u}^\mathrm{S}\, dx + \int_{\partial\Omega_\mathrm{C}} \mathbf{t}^\mathrm{C} : \delta\mathbf{u}^\mathrm{S}\, dx + \int_{\Omega^\mathrm{C}} \rho_0 \mathbf{B}^\mathrm{C} : \delta\mathbf{u}^\mathrm{S}\, dx \right) = 0$$

The system's solution is derived based on the fundamentals of the *Finite Element Method*. As a consequence, a discretization for describing the problem statement has to be introduced. The variation of Eq. (5) w.r.t. the discretization variables δu_r yields the components R_r of the residual force vector.

$$\delta W = \sum \frac{\partial W}{\partial u_r} \delta u_r = \sum R_r \delta u_r = 0 \tag{6}$$

The residual force vector is equal to zero for arbitrary variations. The resulting system of equations can be solved with linearization by the Newton-Raphson method.

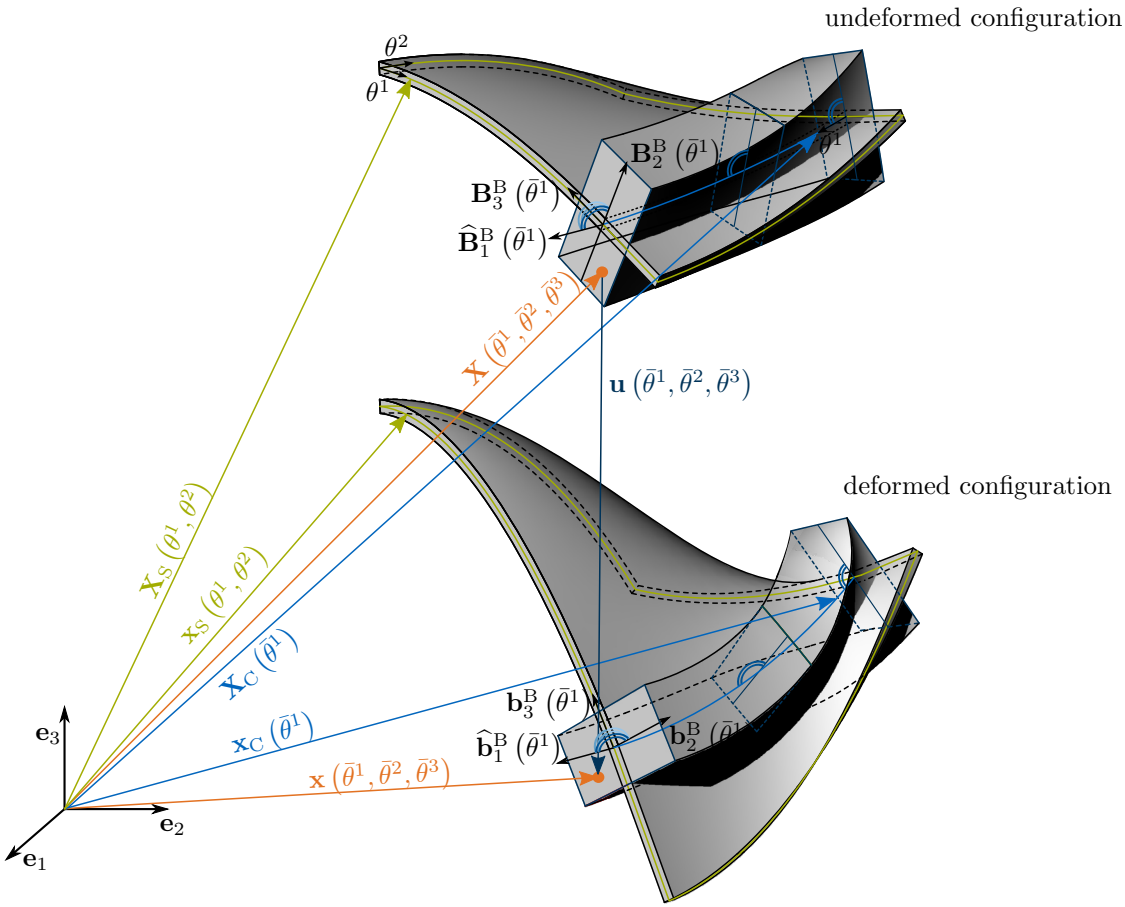

Figure 3: Definition of the position vectors $\mathbf{X}$ and $\mathbf{x}$, the surface vectors $\mathbf{X}_{\mathrm{S}}$ and $\mathbf{x}_{\mathrm{S}}$ and the center line vectors $\mathbf{X}_{\mathrm{C}}$ and $\mathbf{x}_{\mathrm{C}}$ for the undeformed and deformed configuration with a cross section defined by $\mathbf{B}_2^{\mathrm{B}}$ and $\mathbf{B}_3^{\mathrm{B}}$. Here illustrated for a rectangular cross section, which is aligned to the surface normal. Adapted from [11].

The element formulation is deduced from the description of the continuum of the embedded beam. The embedded curve description is used for the center line $\mathbf{X}_{\mathrm{C}}$ and the respective base vectors $\mathbf{B}_2^{\mathrm{B}}$ and $\mathbf{B}_3^{\mathrm{B}}$ for the cross section are derived from the surface

normal (*c.f.* Fig. 3). Capital letters refer in the following to the undeformed configuration whereas lower-case letters denote the deformed configuration. Bernoulli kinematics without warping are assumed.

$$\mathbf{X}\left(\bar{\theta}^1,\bar{\theta}^2,\bar{\theta}^3\right) = \mathbf{X}_{\mathrm{C}}\left(\bar{\theta}^1\right) + \bar{\theta}^2\mathbf{B}_2^{\mathrm{B}}\left(\bar{\theta}^1\right) + \bar{\theta}^3\mathbf{B}_3^{\mathrm{B}}\left(\bar{\theta}^1\right) \tag{7a}$$

$$\mathbf{x}\left(\bar{\theta}^1,\bar{\theta}^2,\bar{\theta}^3\right) = \mathbf{x}_{\mathrm{C}}\left(\bar{\theta}^1\right) + \bar{\theta}^2\mathbf{b}_2^{\mathrm{B}}\left(\bar{\theta}^1\right) + \bar{\theta}^3\mathbf{b}_3^{\mathrm{B}}\left(\bar{\theta}^1\right) \tag{7b}$$

The kinematics are derived straight forward from the continuum by means of fundamentals of continuum mechanics. The respective base vectors are defined as follows:

$$\mathbf{G}_i = \frac{\partial \mathbf{X}}{\partial \bar{\theta}^i} = \mathbf{X}_{,\bar{i}}\,, \qquad \mathbf{g}_i = \frac{\partial \mathbf{x}}{\partial \bar{\theta}^i} = \mathbf{x}_{,\bar{i}} \tag{8}$$

Subsequently, the Green-Lagrange strains can be computed.

$$E_{ij} = \frac{1}{2}\left(g_{ij} - G_{ij}\right) \quad \text{, where } i,j \in \{1,2,3\} \text{ and } G_{ij} = \mathbf{G}_i \cdot \mathbf{G}_j \text{ (analogously: } g_{ij}) \tag{9}$$

Stress and strain fields are linked by the constitutive law $\mathbf{S} = \mathbf{C} : \mathbf{E}$. A detailed specification of the resulting terms of the virtual work, as well for the boundary conditions, can be found in [11].

5 APPLICATION EXAMPLES

In this section, two different application examples are demonstrated. They reveal the advantages and flexibility of the proposed method in the context of architecture and structural design.

5.1 Membrane restrained girder

Alpermann proposed a membrane restrained girder in his PhD thesis [12]. A membrane is inserted between curved beams in order to transfer shear forces. This structural component provides a solution for lightweight and wide-span structures. Additionally, it is stated that the fabrication and transportation is facilitated by elastically bent profiles. The simulation of such structures has to consider staging. Two beams are bent into a curved form and stabilized by a inner membrane and bar spacers. Alpermann uses a circle segment as design objective. In this contribution, a bending shape is additionally examined due to the simpler construction (see Fig. 4).

In the next simulation step, the resulting shape is used for the generation of the slightly prestressed membrane and embedded bar spacers are introduced in order to keep the outer beams in position. The structure, which is in equilibrium for a fixed support on the right, is loaded in a third simulation and the right support is again released in the tangential

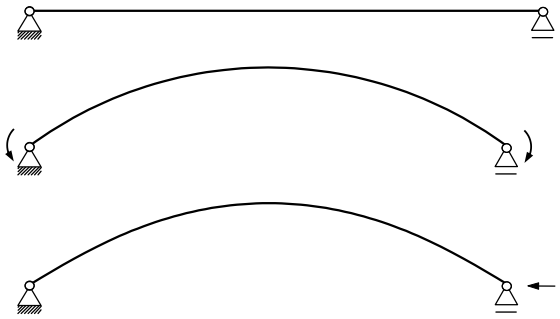

Figure 4: First simulation step for the membrane-restrained girder by Alpermann [12] – shaping the outer profiles.

direction. Embedding the bar spacers into the membrane has in contrast to the conventional explicit modeling the advantage that the design can be easily modified without considering the meshing and coupling of the membrane and the outer beams. Below, several exemplary configurations are examined and illustrated in Fig. 5. Additionally, type A is also computed without considering the first staging step, *i.e.* initially curved beams. This variant is marked with $^{\text{woR}}$.

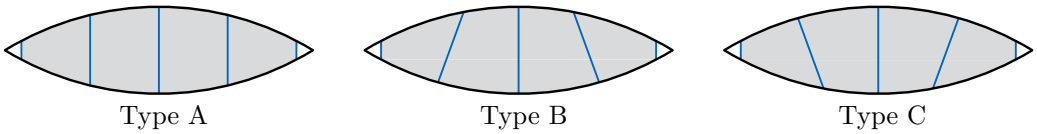

Figure 5: Membrane-restrained girder by Alpermann [12] with elastically bent outer profiles and varied bar spacers.

These design alternatives can be evaluated *e.g.* by the comparison of their behavior under a dead load on the lower outer beam as shown in Fig. 6. The variation study shows different structural responses and proves the benefit of a simple procedure for geometry variation during analysis.

The maximal deformation of the load study presented in Fig. 6 is shown in Fig. 7 for every variant. One observes a different behavior of deformation for the different initial shaping in the first simulation step.

5.2 Batsail

Another field of application within structural design can be seen in the form-finding procedure of hybrid structures. Hybrid structures in this context are prestressed membranes stiffened by elastically bent (bending-active) beams. Such systems provide high efficiency and open up new possibilities for shaping such free form geometries. However, the design procedure of hybrid structures is very complex. There is a high interdependency between form and force due to the low or even non-existing bending stiffness. A

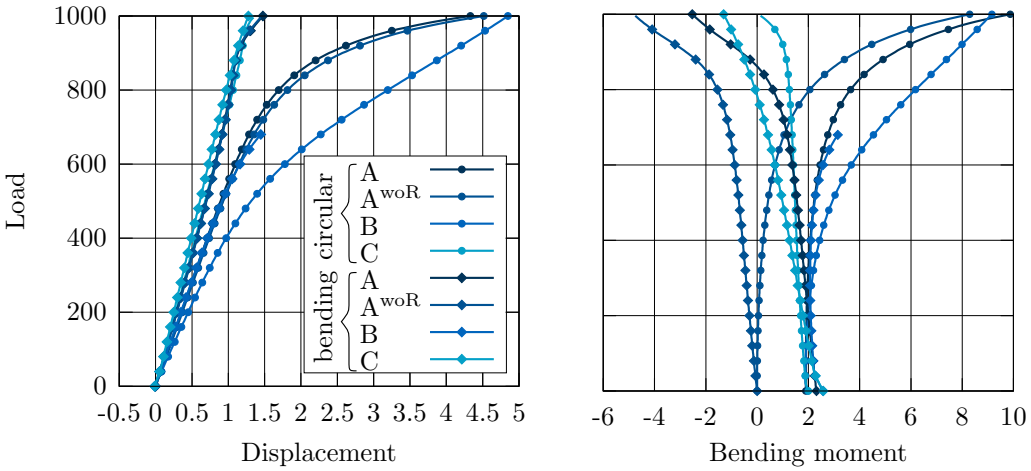

Figure 6: Membrane-restrained girder by Alpermann [12] with elastically bent outer profiles and varied bar spacers. Results for increasing load at the mid point of the lower outer beam for the vertical displacement and the bending moment.

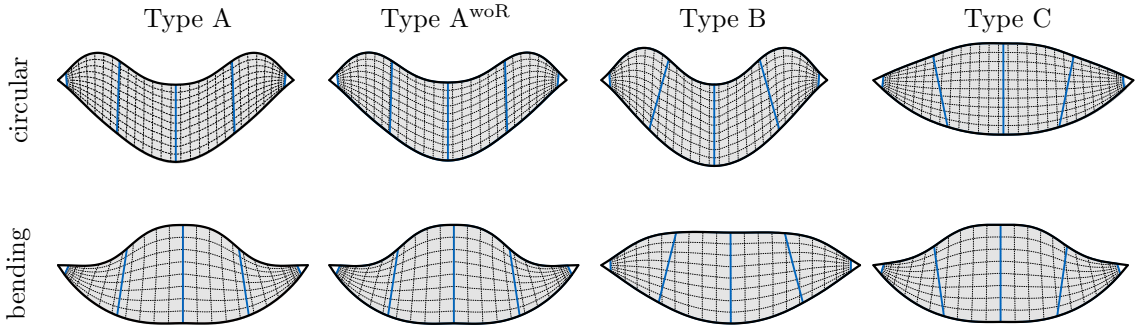

Figure 7: Maximal deformation of the membrane-restrained girder for every variant of the case study.

topology of membranes and cables is given in the classical approach of form-finding. The computation outputs a possible state of equilibrium under a defined force distribution and boundary conditions. The Batsail by Off [13] is chosen as demonstrator example in the following for exemplifying the extended approach. The elastic beams are embedded in the initial topology such that they have their initial length and form (see Fig. 8). Since only the topology has to be modeled for the membrane and cables, it can be modeled flat similar to the projection on the ground. Boundary conditions can be applied subsequently by fixed initial displacements (here for the high points). A deformation of the beam implies inner forces, whereas the initial geometries of the membrane and cables are updated during the form-finding analysis. Note that the initial geometry refers to the stress-free configuration in this contribution.

The initial beams are slightly curved in order to force the buckling into the desired

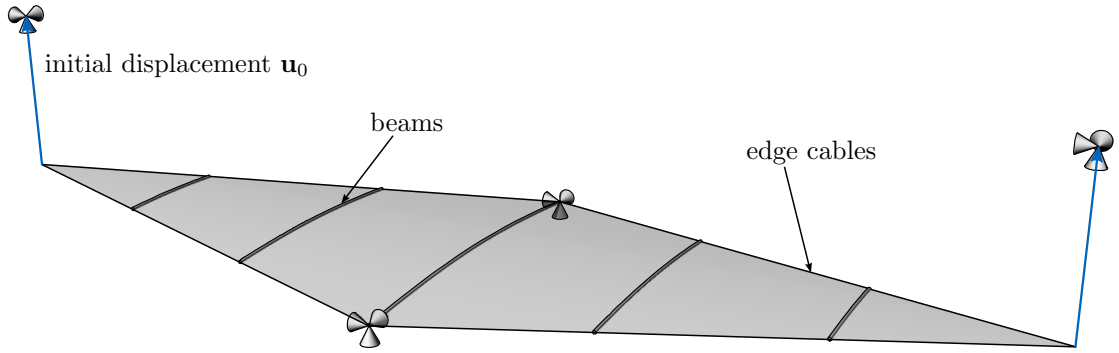

Figure 8: Initial topology with stress-free beams for the form-finding process of the Batsail by Off [13].

direction. Alternatively, forces can be used for controlling the buckling. The length and curvature of the beam are only varied by the forces applied through the membrane or cables. The computational form-finding analysis based on the Updated Reference Strategy (URS) by Bletzinger *et al.* [14] returns for example a solution in equilibrium as shown in Fig. 9.

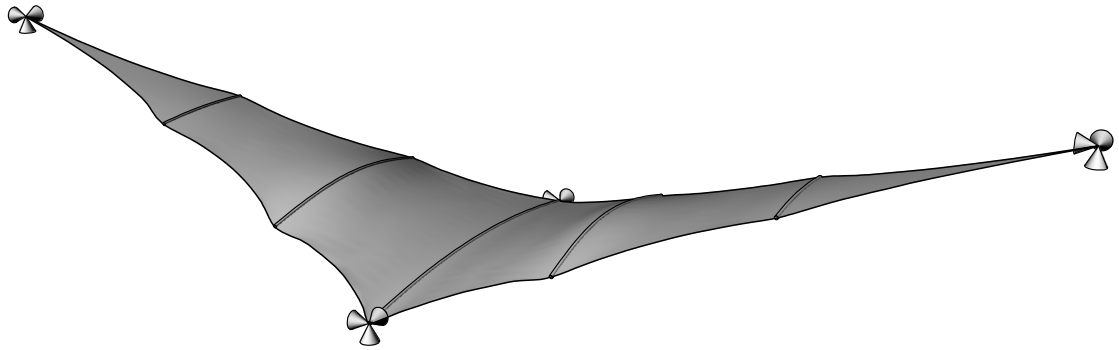

Figure 9: Formfound Batsail by Off [13] with elastically bent beams in equilibrium.

The advantage can be seen in the mesh independent modification of the beams. A study with several variations of the positioning of the beams with the respective parameter space and form-found structure is shown in Fig. 10.

6 CONCLUSIONS

The benefits of isogeometric analysis for staged construction is demonstrated. The advantages can be seen in avoiding the transfer between two frameworks and the consequent loss of result information. Furthermore, embedded entities can be defined independently of the mesh. The embedding technique within NURBS geometries is shown briefly. The application of these embedded geometries for structural analysis is explained shortly by

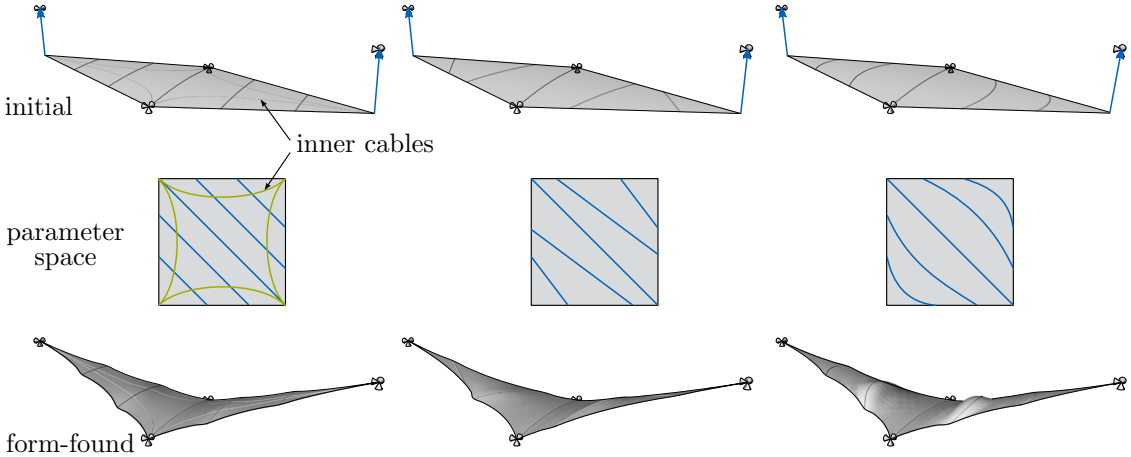

Figure 10: Variations of the Batsail by Off [13] with initial topology, respective parameter space and form-found solution.

using an example of a beam. Two application examples are carried out in order to prove the advantages of embedding in staged construction.

The next step will be to modify the embedding technique within NURBS such that the control points of the embedded entity are also attributed with DOFs. This enables *e.g.* the possibility of a cable that can move on a membrane while staying attached to it. It can be taken even further by nesting another NURBS curve into the parameter space of the surface-embedded curve. Such a description can represent a sliding cable in a sleeve. This would enable the simulation of prestressing during the construction by cables.

REFERENCES

[1] Hughes, T.J.R., Cottrell, J.A. and Bazilevs, Y., Isogeometric analysis: CAD, finite elements, NURBS, exact geometry and mesh refinement. *Comp. Meth. Appl. Mech. and Engng.* (2005) **194**:4135-4195.

[2] Breitenberger, M., Apostolatos, A., Philipp B., Wüchner, R. and Bletzinger, K.-U., Analysis in computer aided design: Nonlinear isogeometric B-Rep analysis of shell structures. *Comp. Meth. Appl. Mech. and Engng.* (2015) **284**:401-457.

[3] Philipp B., Breitenberger, M., D'Auria I., Wüchner, R. and Bletzinger, K.-U., Integrated design and analysis of structural membranes using the Isogeometric B-Rep Analysis. *Comp. Meth. Appl. Mech. and Engng.* (2016) **303**:312-340.

[4] Kiendl, J., Bletzinger, K.-U., Linhard, J. and Wüchner, R., Isogeometric shell analysis with KirchhoffLove elements. *Comp. Meth. Appl. Mech. and Engng.* (2009) **198**:3902-3914.

[5] Dieringer, F., Philipp B., Wüchner, R. and Bletzinger, K.-U., Numerical methods for the design and analysis of hybrid structures. *Int. J. Space Struct.* (2013) **28**:149-160.

[6] Piegl, L. and Tiller, W. *The NURBS book*, in: Monographs in Visual Communication, Springer, 2nd Edition, 1997.

[7] Choi, B.K. *Surface modeling for CAD/CAM*, in: Advances in Industrial Engineering, vol. 11, Elsevier, 1991.

[8] Patrikalakis, N.M., Surface-to-surface intersections. *IEEE Comput. Graph. Appl.* (1993) **13**(1):89–95.

[9] Sederberg, T.W. and Meyers, R.J., Loop detection in surface patch intersections. *Comput. Aided Geom. Des.* (1988) **5**(2):161–171.

[10] Krishnan, S. and Manocha, D., An efficient surface intersection algorithm based on lower-dimensional formulation, *ACM Trans. Graph. (TOG)* (1997) **16**(1):74–106.

[11] Bauer, A.M., Breitenberger, M., Philipp B., Wüchner, R. and Bletzinger, K.-U., Embedded structural entities in NURBS-based isogeometric analysis. *Comp. Meth. Appl. Mech. and Engng.* accepted for publication.

[12] Alpermann, H. *Membranversteifte Tragwerke*. Universität der Künste Berlin, 2015.

[13] Off, R. *New trends on membrane and shell structures - examples of batsail and cushion-belt technologies*. Structures and Architecture Cruz (Ed.), Taylor & Francis Group London, 2010.

[14] Bletzinger, K.-U. and Ramm, E. A general finite element approach to the form-finding of tensile structures by the updated reference strategy. *Int. J. Space Struct.* (1999) **14**(2):131-145.